

MAGLEV - Magnetic Levitation in a Eletromagnetic Suspension System with Eddy Currents

Pedro Almeida
pedro.j.alves.almeida@tecnico.ulisboa.pt

Instituto Superior Técnico, Lisbon, Portugal

January 2021

Abstract

Magnetic Levitation is a field of study whose research is up to date and it poses as a technology with a vast potential in our world. For several reasons, it has been a technology that is not always used, however it can answer many different problems found today in our society. In order to complement the knowledge in this specific area and possibly help spread its application, this thesis analyses different simulation methods of the behaviour of a magnetic levitation system, with the intent to thoroughly study and take advantage of all the benefits it can provide. All the methods studied have different simplified assumptions that facilitate their use and help differentiate them, but all the results obtained, as a consequence, end up with slight variations. Several calculation algorithms are developed that provide the characteristic parameters of the system. These are also obtained with a finite element method model. With this, one can understand how the system works, how the variables behave and all their relations. All these methods are applied to a certain system, the results are compared and many different conclusions are reached. This analysis is fundamental because it helps to understand the system as a whole.

Keywords: Magnetic field, Electromagnetic induction Magnetic Levitation

1. Introduction

Magnetic levitation is a topic that is unknown to the general public. Usually, only people that study it acquire knowledge about it, even though it has a wide range of applicability in our society. To increase and expand this technology there has to be a deep study about it.

In this article, several methods that simulate the behaviour of a magnetic levitation system will be examined and applied in order to understand how such a system can be used and to take advantage of all its benefits. All the methods consider several simplifying hypotheses that facilitate the equations behind the behaviour of the system and help understand how the characteristic parameters vary with each variable. All the methods consist of a coil carrying a time-varying current that levitates above a conducting sheet. The current has a frequency equal to 50 Hz and has a uniform distribution along the cross section of the coil.

In the first method analysed, present in [5], the author considers that the conducting sheet is perfect and has infinite thickness, which means, the losses in the conducting sheet are equal to zero. The coil has a circular cross section This approximation is an oversimplification of the problem, even though

it facilitates the calculations.

Afterwards, the methods present in [4] and [7] were studied. Both these methods approach the problem in a similar manner. In contrast with the previous method, these ones consider the losses and a finite thickness regarding the conducting sheet. The differences are that in [4] the cross section is circular whereas in [7] the cross section is rectangular. In the latter, the inductance is given by its exponential approximation.

All these three methods consider the problem as a two dimension planar configuration and each respective author calculates every variable per unit.

Finally, the last method that is studied is present in [3], which considers a circular cross section with a conducting sheet with finite conductivity and finite thickness. The main difference between this method and all the others is that this author uses an axisymmetric configuration.

The methods discussed previously are used to calculate the value of the magnetic field in the various regions of the systems and from this value the induction coefficient of the coil and the levitation force are found. Calculation, practical and simulation methods are used and its results are compared so that conclusions can be reached in order to increase

the knowledge of this technology.

Simulation and calculation methods help understand the reality of magnetic levitation systems without the need for practical trials.

2. Description of the used methods

2.1. Planar Configuration

The first method that was studied in order to develop this article is present in [5]. The author considers a conducting sheet with infinite thickness and infinite conductivity. Assuming all the simplifying hypotheses previously mentioned and present in the article cited, the value of the inductance can be given by

$$L_n = \frac{\mu_r}{2} + 2 \ln \left(\frac{2h_c d}{r_0 \sqrt{d^2 + h_c^2}} \right), \quad (1)$$

where μ_r is the relative permeability of the material, h_c the distance between the center of the conductor of the coil and the conducting sheet, d the distance between the center of the conductor of the coil and the center of the coil (radius of the coil), and, finally, r_0 the radius of the conductor of the coil.

The normalization used in the previous equation is equal to

$$L_{norm} = \frac{\mu_0}{2\pi} N^2 l, \quad (2)$$

with l equal to the coil length and N the number of turns in the coil.

Using the virtual work principle through the derivative of the system inductance coefficient for varying height of the coil in relation to the conducting sheet it is possible to calculate the value of the normalized magnetic force, which is given by

$$F_n = \frac{2}{\frac{h_c}{r_0} \left[1 + \left(\frac{h_c}{d} \right)^2 \right]}. \quad (3)$$

The normalization used for the force is

$$F_{norm} = \frac{1}{2} I_{coilrms}^2 \frac{\mu_0}{2\pi r_0} N^2 l, \quad (4)$$

where I_{bef} is the root mean square value of the current in the coil.

A *MATLAB* [6] routine, named *placaperf.m*, was developed using the equations formerly mentioned to simulate and further understand the behaviour of a magnetic levitation system. The results present in this article were obtained using this routine.

An approximation to reality was made and the conducting sheet was considered to have finite conductivity and finite thickness. These hypotheses are present in [4] and [7], the former being a theoretical approach and the latter a practical approach.

The author from [4] is able to reach a value for the normalized inductance, considering all the simplifying hypotheses mentioned

$$L_n = L_{psn} + L_{csn}, \quad (5)$$

where L_{psn} corresponds to the inductance for the perfect sheet case and L_{csn} corresponds to the inductance for the conducting sheet with finite conductivity case.

L_{psn} is already present in (1), since this contribution is exactly the same as the case discussed in [5].

When finite conductivity is considered, a correction must be done, so the value of this correction is equal to

$$L_{csn} = 8Re \left[\int_0^{+\infty} V(\xi) e^{-2h_{cn}\xi} \sin^2(\xi d_n) d\xi \right], \quad (6)$$

with

$$V(\xi) = \frac{1}{\sqrt{\xi^2 + j}} \frac{\cosh(v) + \beta \sinh(v)}{2\beta \cosh(v) + (\beta^2 + 1) \sinh(v)}, \quad (7)$$

$$\beta = \frac{|\xi|}{\sqrt{\xi^2 + j}}, \quad (8)$$

$$v = \sqrt{\xi^2 + j} t_n. \quad (9)$$

h_{cn} is equal to the normalized distance between the center of the conductor of the coil and the conducting sheet, d_n is equal to the normalized distance between the center of the conductor of the coil and the center of the coil (radius of the coil) and, finally, t_n is equal to the normalized thickness of the conducting sheet.

The normalization used for the inductance is equal to (2). The other values obtain are normalized with a multiplication by a factor q , equal to

$$q = \frac{\sqrt{2}}{\delta}, \quad (10)$$

where δ is the penetration depth

$$\delta = \sqrt{\frac{2}{\omega \mu \sigma}}, \quad (11)$$

in a medium with permeability μ and conductivity σ . ω corresponds to the value of angular frequency.

The magnetic force is given by

$$F_n = \frac{F_{av}}{F_{norm}}, \quad (12)$$

with

$$F_{norm} = \frac{1}{2} \frac{\mu_0 l I_{coilrms}^2 N^2}{2\pi r_1}, \quad (13)$$

and

$$F_{av} = \frac{1}{2} I_{coilrms}^2 \frac{\partial L}{\partial h}. \quad (14)$$

$I_{coilrms}$ is equal to the value of the current in each turn of the coil and l is the length of the coil.

By contrast, the author in [7] considers the exponential approximation of the inductance, which is the following

$$L = L_0 - L_r e^{-\frac{h}{\gamma}}, \quad (15)$$

L_0 represents the terminal inductance (value of the inductance when the height of the coil is equal to infinity). L_r describes the way the value of the inductance lowers when it comes closer to the conducting sheet. The γ is the attenuation factor, as described in [7].

In order to study and understand the method described, a *MATLAB* routine named *placaimperf.m* was developed, where this method is recreated using the equations present in this section.

2.2. Axisimetric Configuration

To analyse this configuration two articles were studied, [3] and [2]. The main difference between them is that the author in [2] considers the conducting sheet to have infinite thickness and advocates that considering the value of the thickness in the calculations is not an adequate method since it adds on complexity and the final result only deviates 3 %, in the cases it was applied, which in his opinion is not worth the effort. The author in [3] takes the value of the thickness of the conducting sheet into account.

In [3], the author considers a system that is symmetric to a vertical axis, so despite being a three-dimensional system, only two coordinates are needed (radius and height) to calculate all the characteristic parameters, which helps understand the behaviour of the system as a whole. With the help of Bessel functions, the author is able to calculate the value of the potential vector of the magnetic field in every region of the system. From this value, he is capable of reaching the value of the impedance of the system and thereafter the values of the inductance, losses and magnetic force, which allow a full understanding of the system as a whole.

2.3. Simulation Using a Finite Element Method

Finally, to compare the results and help validate the methods previously described, the program *FEMM* [1] was used. The finite element method is important because it solves differential equations numerically. This particular case serves as a tool to find the value of the magnetic field. It poses as a versatile and rigorous simulation program.

3. Results

3.1. Planar configuration

The *placaperf.m* algorithm was applied to the following data set

- relative permeability $\mu_r = 1$;
- radius of the conductor in the coil $r_0 = 10 \text{ mm}$;
- distance from the center of the conductor to the center of the coil $d = 40 \text{ mm}$;
- number of turns $N = 100$;
- axial length $l = 100 \text{ mm}$;
- resistance of the coil $R = 0,38 \text{ }\Omega$;
- weight of the coil $mg = 3,5 \text{ N}$.

The values of the inductance of the coil and force in relation to h_c/r_0 are present in Figures 1 and 2.

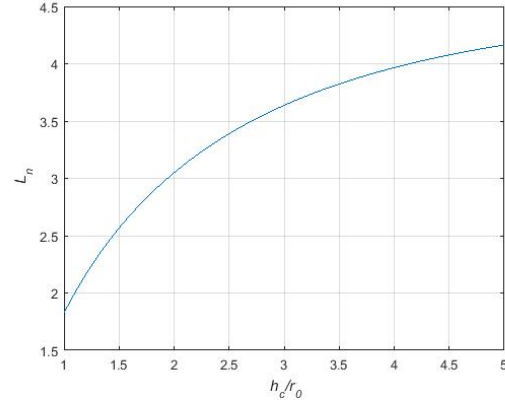


Figure 1: Normalized inductance in relation to the height of the coil dividing by the radius of the conductor in the coil.

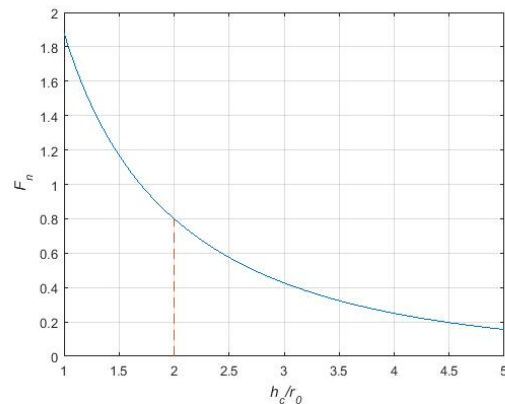


Figure 2: Normalized force in relation to the height of the coil dividing by the radius of the conductor in the coil.

The first conclusion to take from the results obtained is that the value of the inductance increases when the value of the height increases whereas the value of the force decreases when the value of the height increases. A point of equilibrium was found when the force equals the value of the weight of the coil, for a height of $h_c = 2r_0 = 20 \text{ mm}$, present in the Figure 2 in the dashed vertical line.

To apply the previously mentioned algorithm *placaimperf.m* to the system, the upcoming data set was used

- radius of the conductor in the coil $r_1 = 10 \text{ mm}$;
- distance from the center of the conductor to the center of the coil $d = 40 \text{ mm}$;
- thickness of the insulator in the conductor of the coil $e = 2 \text{ mm}$;
- height of the coil $h_c = 22 \text{ mm}$;
- number of turns $N = 107$;
- thickness of the conducting sheet $t = 10 \text{ mm}$;
- axial length $l = 91,9 \text{ mm}$;
- resistance of the coil $R = 0,38 \ \Omega$;
- frequency $f = 50 \text{ Hz}$;
- current in each turn $I_{coilrms} = 26,8 \text{ A}$.

The results obtained from this algorithm are present in the Figures 3 to 10.

In Figure 3 the values of the normalized magnetic induction in relation to the position dividing by the height of the coil are present.

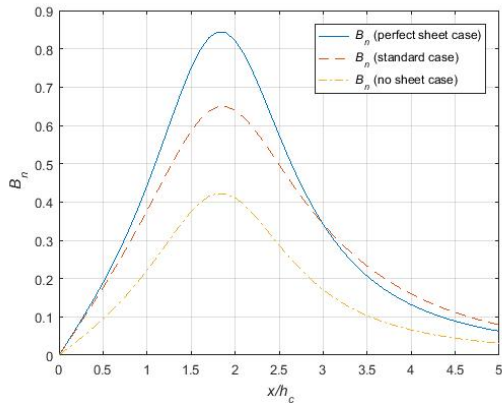


Figure 3: Normalized magnetic induction (B_n) in relation to the position dividing by the height of the coil (x/h_c)

In this figure, the effect of the consideration of a conducting sheet with finite conductivity is evident

in comparison with the case considering a perfect sheet

In Figure 4 the values of the normalized inductance in relation to the frequency are shown. It is possible to understand that the inductance decreases with the increase of the frequency, even though it tends to stabilize its value.

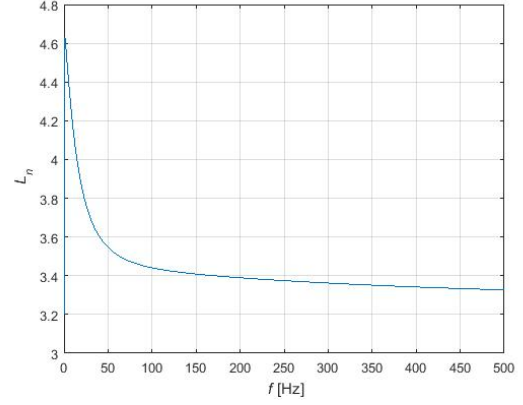


Figure 4: Normalized inductance of the coil in relation to the frequency.

In Figures 5, 6 and 7 are shown the values of the normalized inductance, normalized force and normalized losses, respectively, in relation to the normalized height of the coil. In Figure 5 are present different curves, the dashed one corresponds to the case when the conducting sheet is considered perfect, the dashed-dotted line corresponds to the correction of the consideration of a conducting sheet with finite conductivity and thickness. Lastly, the solid line corresponds to the standard case, which is the result of the sum of the two cases previously mentioned.

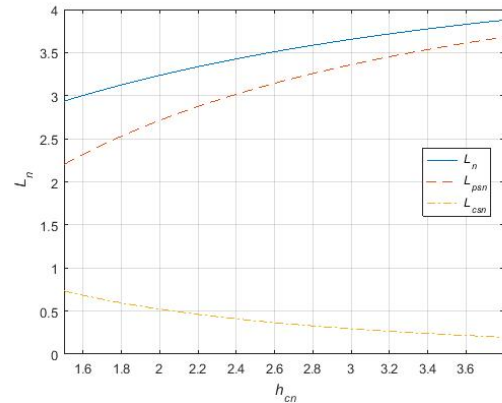


Figure 5: Normalized inductance of the coil in relation to the normalized height, $h_{cn} = qh_c$.

In Figure 6 is not only shown the values of the normalized force but also the effect of an exponen-

tial approximation to calculate the inductance and its consequences on the values of force. The formula to calculate the inductance, present in [7] is given by (15), where

- $L_0 = 980 \mu H$
- $L_r = 358 \mu H$
- $\gamma = 22 \text{ mm}$

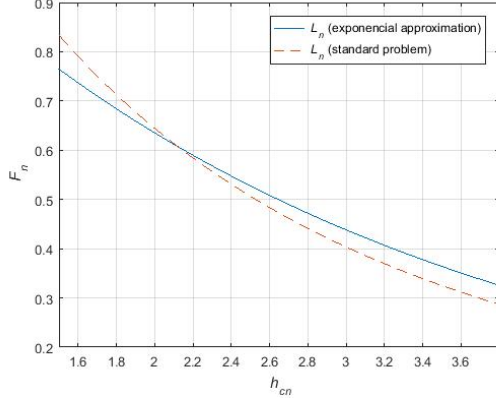


Figure 6: Normalized force in relation to the normalized height.

It is possible to observe in Figure 6 that the results obtained with this approximation do not drift away from the ones obtained without it.

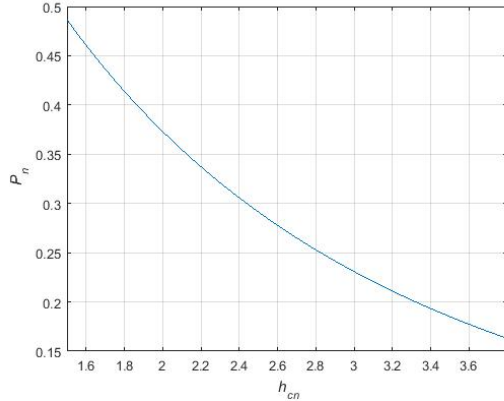


Figure 7: Normalized Joule losses in relation to the normalized height.

In Figure 7, the normalization used is equal to

$$P_{norm} = \frac{lI_{coilrms}^2 N^2}{\pi \sigma r_1^2}. \quad (16)$$

In Figures 8, 9 and 10 are present the values of the normalized inductance, normalized force and normalized losses, respectively, in relation to the normalized thickness of the conducting sheet. In Figure 8 the dashed line corresponds to the values of

the perfect sheet case, which is, as expected, a constant, since the thickness of the conducting sheet is irrelevant. The dashed-dotted line corresponds to the correction of the consideration of a conducting sheet with finite conductivity and thickness and the solid line shows the values of the standard case.

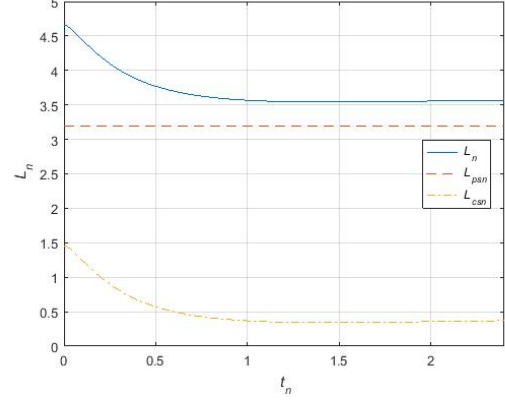


Figure 8: Normalized inductance of the coil in relation to the normalized thickness of the conducting sheet.

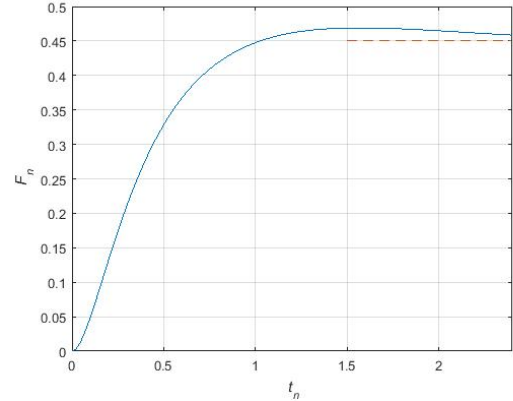


Figure 9: Normalized force in relation to the normalized thickness of the conducting sheet.

In Figures 9 and 10 the dashed line represents the value when the conducting sheet is considered to have infinite thickness, as in [2]. It is possible to conclude that this approximation is valid when the value of the thickness is high.

In order to compare both approximations discussed it was considered a coil height of $h_c = 22 \text{ mm}$ and the results in Table 1 were obtained.

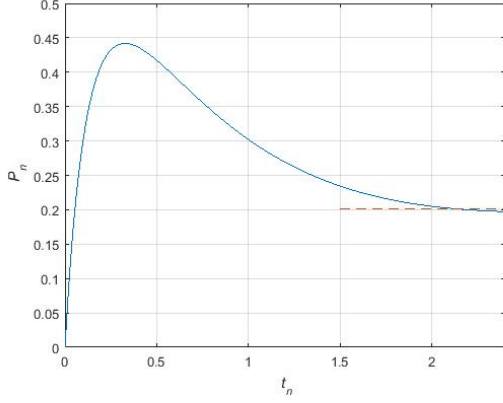


Figure 10: Normalized losses in relation to the normalized thickness of the conducting sheet.

	perfect conducting sheet	sheet with finite conductivity
$I_{coilrms} [A]$	22,4	26,8
$P_{joule} [W]$	190,6	273 + 16,8

Table 1: Comparison of a system with a perfect conducting sheet and a system with a conducting sheet with finite conductivity.

The values of the losses, in the case of the sheet with finite conductivity, correspond to the losses in the coil (273 W) and the losses in the conducting sheet (16,8 W). In the case of the perfect conducting sheet, the value shown is for the losses in the coil, as the sheet is perfect and does not have losses.

3.2. Validation of the results obtained with planar configuration

In order to validate the results obtained with the algorithm *placaimperf.m* the same system was applied in *FEMM*. Both methods used the same data set:

- radius of the conductor in the coil $r_1 = 10 \text{ mm}$;
- distance from the center of the conductor to the center of the coil $d = 40 \text{ mm}$;
- height of the coil $h_c = 22 \text{ mm}$;
- number of turns $N = 100$;
- thickness of the conducting sheet $t = 10 \text{ mm}$;
- current in the coil $I_{coilrms} = 1 \text{ A}$;
- axial length $l = 92 \text{ mm}$.

A boundary condition was set in *FEMM*, a circle with a radius of 1000 mm centered in the system and the *mesh size* was set to 3 mm in the coil and

conducting sheet and 10 mm for the rest of the space which is considered air.

The inductance calculated with *placaimperf.m* is

$$L_{calc} = 7,46 \times 10^{-4} H. \quad (17)$$

The inductance using *FEMM* is equal to

$$L_{sim} = 7,62 \times 10^{-4} H. \quad (18)$$

Both this values are in the same order of magnitude. The values of the magnetic induction on the surface of the conducting sheet are present in Figure 11.

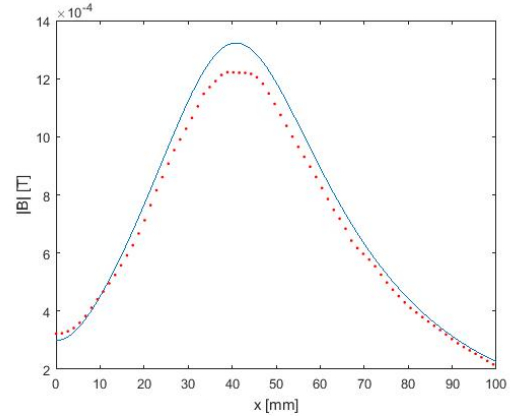


Figure 11: Magnetic induction on the surface of the conducting sheet, for different values of x, using *FEMM* (points) and the algorithm (line).

Finally, the force calculated with *placaimperf.m* is

$$F_{calc} = 0,00425 N. \quad (19)$$

The force using *FEMM* is equal to

$$F_{sim} = 0,00414 N. \quad (20)$$

The conclusion drawn from the analysis of the results obtained is that both method used reach approximately the same results, therefore the numeric method in [4] is validated.

3.3. Influence of the cross section in a axisymmetric configuration

The systems present in [4] and [7] are applied in *FEMM* with the difference that the axisymmetric configuration is considered for both of them.

The system with circular cross section has the following dimensions

- radius of the conductor in the coil $r_1 = 10 \text{ mm}$;
- distance from the center of the conductor to the center of the coil $d = 40 \text{ mm}$;

- height of the coil $h_c = 22 \text{ mm}$;
- number of turns $N = 100$;
- thickness of the conducting sheet $t = 10 \text{ mm}$;
- current in the coil $I_{coilrms} = 1 \text{ A}$.

And the system with rectangular cross section has the following dimensions

- interior radius of the coil $r_1 = 31,14 \text{ mm}$;
- exterior radius of the coil $r_2 = 48,86 \text{ mm}$;
- distance from the center of the conductor to the center of the coil $d = 40 \text{ mm}$;
- inferior height of the coil $l_1 = 10 \text{ mm}$;
- superior height of the coil $l_2 = 27,72 \text{ mm}$;
- number of turns $N = 100$;
- thickness of the conducting sheet $t = 10 \text{ mm}$;
- current in the coil $I_{coilrms} = 1 \text{ A}$.

In this case, the boundary condition was a semi-circle with 1000 mm radius.

The inductance obtained with a circular cross section is equal to

$$L_{sim} = 7,64 \times 10^{-4} H. \quad (21)$$

While the value of the inductance obtained with a rectangular cross section is

$$L_{sim} = 7,27 \times 10^{-4} H. \quad (22)$$

In Figure 12 it is possible to observe the values of the magnetic induction on the surface of the conducting sheet for both systems.

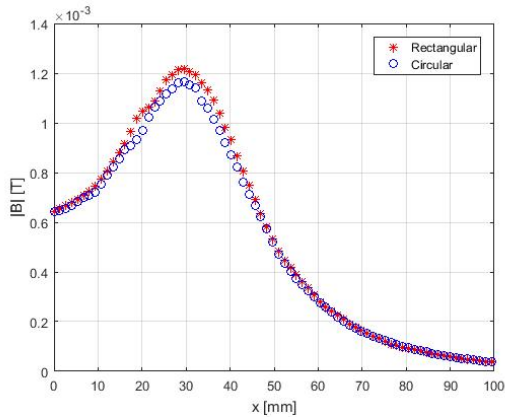


Figure 12: Magnetic induction on the surface of the conducting sheet, for circular and rectangular cross sections.

For a constant value of current the values of the Tables 2 and 3 were obtained. These tables show the values of inductance and force for different heights of the coil in the cases of a rectangular cross section and circular cross section.

Height [mm]	Inductance [μH]	Force [N]
12	669	0,00696
22	764	0,00320
32	810	0,00161

Table 2: Inductance and force for different values of height of the coil, with circular cross section.

Height [mm]	Inductance [μH]	Force [N]
12	614	0,00904
22	727	0,00404
32	788	0,00180

Table 3: Inductance and force for different values of height of the coil, with rectangular cross section.

The variations found in the values above can be explained by the differences in the value of the cross section area and the radius of the coil.

3.4. Translation from a planar system to an axisymmetric system

Results for the method present in [3] are not shown due to the fact that the author does not provide the means to verify the results obtained.

In this section two similar systems are simulated in *FEMM* where the only difference between them is the configuration. One is planar whereas the other is axisymmetric. The objective is to find a relation between both this system in order to obtain the same results. The data set to simulate the systems is the following

- radius of the conductor in the coil $r_1 = 10 \text{ mm}$;
- distance from the center of the conductor to the center of the coil $d = 40 \text{ mm}$;
- height of the coil $h_c = 22 \text{ mm}$;
- number of turns $N = 100$;
- thickness of the conducting sheet $t = 10 \text{ mm}$;
- current in the coil $I_{coilrms} = 1 \text{ A}$.

The axial length of the planar system is equal to 92 mm .

In Figure 13 are shown the values of the magnetic induction on the surface of the conducting sheet, for both configurations mentioned.

In Figures 14 and 15 are present the values of inductance and force for different values of height of the coil.

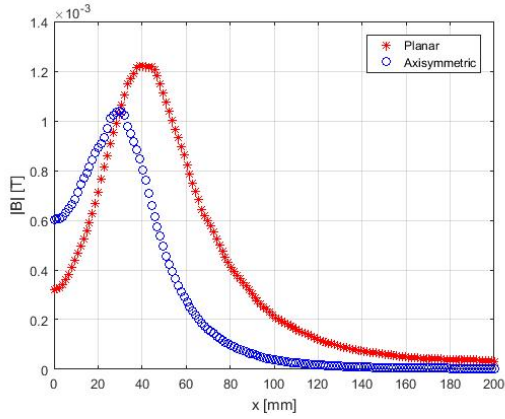


Figure 13: Magnetic induction on the surface of the conducting sheet, for planar and axisymmetric systems, with $d = 40$ mm.

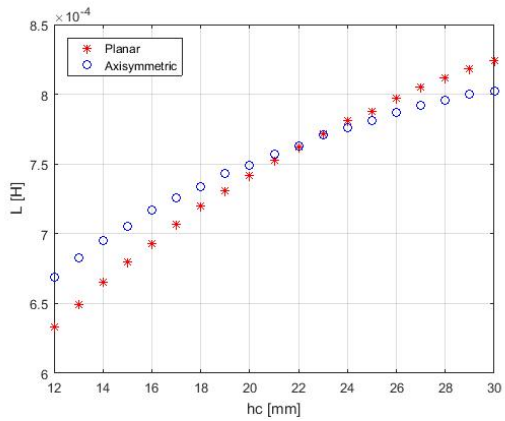


Figure 14: Inductance in relation to the height of the coil, for planar and axisymmetric systems, with $d = 40$ mm.

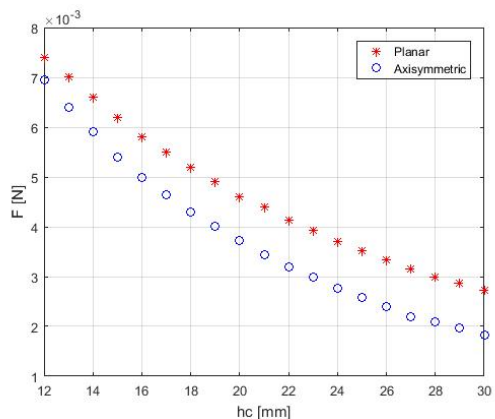


Figure 15: Force in relation to the height of the coil, for planar and axisymmetric systems, with $d = 40$ mm.

In order to approximate the systems, the value of

the distance from the center of the conductor to the center of the coil (d) was adjusted to 55 mm for the axisymmetric case. The magnetic induction on the surface of the conducting sheet is present in Figure 16

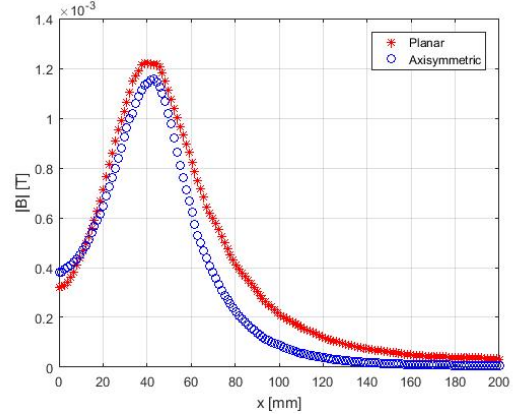


Figure 16: Magnetic induction on the surface of the conducting sheet, for planar system, with $d = 40$ mm, and axisymmetric, with $d = 55$ mm.

When the adjustment to the value of d , in the axisymmetric configuration, is made, the values of the magnetic field for both cases become similar. In Figures 17 and 18 are the values of inductance and force in relation to the height of the coil, for this specific case.

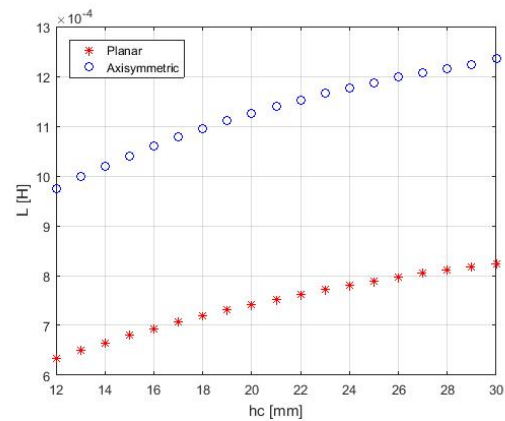


Figure 17: Inductance in relation to the height of the coil, for planar system, with $d = 40$ mm, and axisymmetric, with $d = 55$ mm.

The values of inductance and forces actually deviate from each other which results in the conclusion that the value of the magnetic induction in the surface of the conducting sheet is not an acceptable indicator to compare systems.

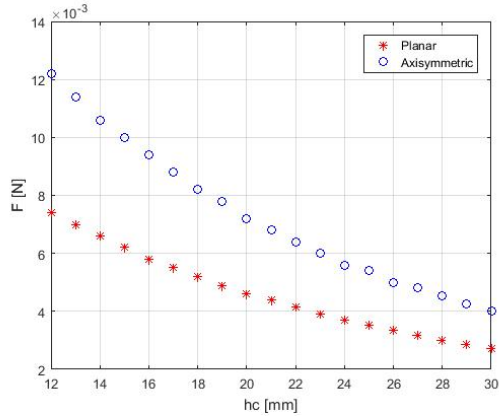


Figure 18: Force in relation to the height of the coil, for planar system, with $d = 40$ mm, and axisymmetric, with $d = 55$ mm.

4. Conclusions

The main objective of this article was to analyse, study and understand different methods of simulating the behaviour of a magnetic levitation system and to find an algorithm that is faster when faced with reduced computational capacities. Therefore, every simplifying hypothesis and its impact on the system were carefully examined.

From the application of the algorithm called *placaperf.m* it is possible to conclude how the inductance and force vary in relation to the height of the coil, the former increases and the latter decreases. From the application of the algorithm called *placaimperf.m* it is possible to understand the behaviour of others parameters of the system and also to understand the behaviour of the system when the thickness of the conducting sheet is considered. When the results of this two algorithms are compared with the results of the practical application in [7] it is possible reach the conclusions that, the method in [5], which considers a perfect conducting sheet, deviates from the real case, due to its simplifying hypothesis, however, it is possible to understand the fundamental laws of the system from it. The method in [4] is more broad and its results are closer to the real case. It is also a more versatile method since it is possible to consider different simplifying hypotheses, depending on the data set used.

Afterwards, *FEMM* was used to validate all the results obtained with the algorithms previously mentioned. The results obtained with *FEMM* are on the same order of magnitude as the ones obtained with the algorithms developed.

FEMM was also used to study the impact of the cross section in the results. A circular and a rectangular cross section were used and the results were moderately different, but this difference can be ex-

plained by the difference in the area of the cross section. The final conclusion is that there was no evidence to support an effect on the results caused by the shape of the cross section.

Finally, *FEMM* was used to find a relation between the planar and the axisymmetric configurations. It is evident in the results present in the article that this relation does not exist. When some variables approximate in both configurations, other variables diverge at the same time, making it impossible to find a relation. But it is possible to correlate each variable independently for both configurations.

While analysing all the results presented in this article it is possible to reach the conclusion that the method present in [4] and developed in the *MATLAB* routine called *placaimperf.m* is the most versatile and broad of them all, being the best method to fully understand the behaviour of the system as a whole. The accuracy of its results is supported by the simulation of the system with *FEMM*.

References

- [1] Femm. in <http://www.femm.info/wiki/HomePage>.
- [2] M. S. Adler. A field-theoretical approach to magnetic induction heating of thin circular plates. *IEEE*, 1974.
- [3] C. V. Dodd and W. E. Deeds. Analytical solutions to eddy-current probe-coil problems. *Journal of Applied Physics*, 1968. doi: 10.1063/1.1656680.
- [4] V. M. Machado. Analytical approach for an ems eddy current maglev problem. *IST*, 2013.
- [5] V. M. Machado. Levitação magnética (maglev) num sistema de suspensão eletromagnética (ems) com correntes turbilhonares. *IST*, 2019.
- [6] MATLAB. *version 9.0 (R2016a)*. The MathWorks Inc., Natick, Massachusetts, 2016.
- [7] M. T. Thompson. Eddy current magnetic levitation: models and experiments. *IEEE*, 2000.